ChemComm

Efficient Cellular Uptake of Click Nucleic Acid Modified Proteins

Journal:	*ChemComm*
Manuscript ID	CC-COM-12-2019-009401.R2
Article Type:	Communication

COMMUNICATION

Efficient Cellular Uptake of Click Nucleic Acid Modified Proteins

Albert Harguindey,[a] Heidi R. Culver,[a] Jasmine Sinha,[a] Christopher N. Bowman,[a,b] Jennifer N. Cha[a,b†]

Received 00th January 20xx,
Accepted 00th January 20xx

DOI: 10.1039/x0xx00000x

Efficient intracellular delivery of biomacromolecules such as proteins continues to remain a challenge despite its potential for medicine. In this work, we show that mScarlet, a non cytotoxic red fluorescent protein (RFP) conjugated to Click Nucleic Acids (CNA), a synthetic analog of DNA, undergo cell uptake significantly more than either native proteins or proteins conjugated with similar amounts of DNA in MDA-MB-468 cells. We further demonstrate that the process of cell uptake is metabolically driven and that scavenger receptors and caveolae mediated endocytosis play a significant role. Co-localization studies using anti-scavenger receptor antibodies suggest that scavenger receptors are implicated in the mechanism of uptake of CNA modified proteins.

The efficient intracellular delivery of biomolecules, including nucleic acids and proteins, has the potential to impact a diverse array of biological and medical applications, including gene editing, protein therapy, imaging and manipulation of cellular activities.[1–8] However, due to their size and charge, it has been challenging to deliver large biomacromolecules into cells while escaping or bypassing the endocytic-lytic pathway. Different strategies to deliver proteins have been studied to overcome these barriers, including nanoparticle encapsulation,[9–15] complexation of proteins to polymers,[12,13] and utilization of cell penetrating peptides or viral vectors.[16–20] Still, important challenges remain, including inefficient release of proteins from their vehicles, poor cell-selective uptake, and insufficient nanoparticle, or protein endosomal escape into the cytosol.[21–23] While supercharged proteins[24] have also been explored as ways to induce cell uptake of biomacromolecules, this approach may not be universal because many proteins are not amenable to such extensive mutagenesis or modification.[25,26] Lastly, methods to introduce proteins using physical insertion methods such as microinjection or electrical pulses often lead to reduced cell viability and poor transfection efficiency.[27,28] More recently, Mirkin and coworkers demonstrated efficient intracellular protein uptake by building a dense corona of negatively charged DNA around proteins known as spherical nucleic acids (SNAs).[29–33] Since linear DNA cannot penetrate cells, the 3D corona of DNA around nanoparticles and proteins is thought to be responsible for driving cell uptake. In addition, extensive work with gold nanoparticle SNAs showed that the cell uptake is metabolically driven and associated with scavenger receptor A (SR-A) binding, indicating that protein uptake is driven by caveolae dependent endocytosis.

The results shown by Mirkin and coworkers led us to investigate biomacromolecular delivery using a synthetic analog of DNA known as click nucleic acids, or CNAs.[9,34–38] First developed by Bowman and coworkers, click nucleic acids (CNAs) are a new family of synthetic analogs of DNA that are produced by thiol-X click chemistry.[34] While CNA is similar to other synthetic nucleic acids like PNA (Peptide Nucleic Acids) with respect to its uncharged backbone, CNA can be easily polymerized into homopolymers and solubilized in certain organic solvents, enabling its incorporation into synthetic polymers typically utilized for drug delivery such as the FDA-approved poly(lactic-*co*-glycolic acid) (PLGA). Using this property, we recently demonstrated the use of CNA to co-deliver DNA, DNA-conjugated prodrug enzymes, and chemotherapy agents into cells by synthesizing and using PEG-CNA-PLGA nanoparticles as delivery vehicles.[9,35] In addition, PEG-CNA polymers were synthesized which showed efficient cell uptake via a passive mechanism.[46]

In this work we studied the effect of conjugating CNA oligonucleotides to proteins on cell uptake, for this we firstly attached polyA and polyT CNA strands to the model protein, mScarlet, a variant of red fluorescent protein (RFP).[39] this protein possesses a high quantum efficiency, and has emission and excitation wavelengths that can be easily tracked by flow cytometry and confocal microscopy.[39] First, standard protein engineering was used to produce His-tagged RFP in *E. coli* and purified. Next, to conjugate polyA and polyT versions of both CNA and DNA to the RFP, the protein was initially reacted with 20 molar equivalents of NHS-DBCO overnight. The DBCO modified RFP were reacted with 5 molar equivalents of the azido-modified DNA (sourced from IDT) or CNA.

[a] Department of Chemical and Biological University of Colorado, Boulder.
[b] Materials Science and Engineering Program, University of Colorado, Boulder

†To whom email correspondence should be addressed: Jennifer.Cha@colorado.edu

Electronic Supplementary Information (ESI) available: [The supplementary information contains detailed materials and methods, the MTT assay for the toxicity if the oligomer-protein conjugates used in this study (Figure S1) as well as the toxicity assays for the Methyl-β-cyclodextrin (Figure S5), Fucoidan (Figure S6), Nystatin (Figure S7) and Chlorpromazine (Figure S8). The SI also includes the Over time delivery of modified proteins in CaCo2 cells (Figure S2), the PAGE of the TAT protein conjugates (Figure S3) and the over time delivery of delivery with these TAT conjugates (Figure S4)]. See DOI: 10.1039/x0xx00000x

The azido-terminated CNA was produced by reacting the thiol terminated CNA were with iodo-PEG3-azide and cleaned by dialysis against DMSO. The final protein conjugates were then characterized by a combination of SDS PAGE and UV-Vis spectroscopy (Figure 1).

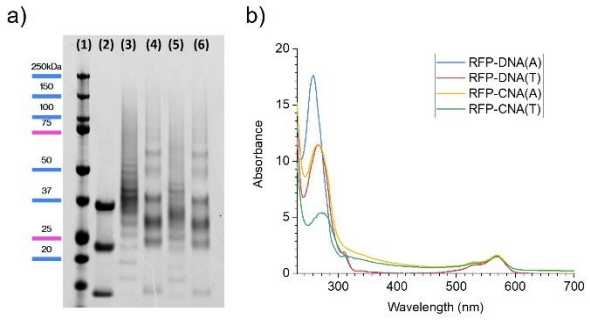

Figure 1. a) SDS-PAGE gel showing successful conjugation of CNA and DNA oligonucleotides to RFP. From left to right: (1) Ladder, (2) unmodified protein, (3) RFP-DNA poly A, (4) RFP-CNA poly A, (5) RFP-DNA poly T, (6) RFP-CNA poly T. b) UV Vis absorption spectra of DNA and CNA conjugated RFP.

As shown in Figure 1a, after reacting azido-DNA or azido-CNA with the DBCO modified RFP, SDS-PAGE showed discrete bands that ran slower than the bands of the native protein. The unmodified RFP runs as three discrete bands corresponding to approximately 14, 23 and 35 kDa, which is thought to correspond to RFP fractions without and with chromophore and the full protein respectively. After nucleic acid conjugation, a recurrent pattern of slower moving bands was observed for both the DNA and CNA modified RFP. Since DBCO modifications and DNA or CNA attachment are random, a range of oligonucleotides is expected to conjugate to each protein. In addition, the CNA strands as synthesized have some degree of polydispersity[39] so fewer discrete bands may be expected with CNA conjugated proteins compared to the DNA-RFP. Assuming the extinction coefficient of CNA is approximately that of the same DNA sequence and length, it was determined that an average of ~4.9 and ~5.4 polyA and polyT DNA strands, respectively, were attached per protein, as compared to ~3.1 and ~2.9 polyA and polyT CNA strands were attached per protein.

Prior to cell uptake studies of the modified proteins, the toxicity of the CNA and DNA modified RFP was first measured and compared to native RFP. For this, 10^3 MDA-MB-468 cells were seeded per well in a 96 well plate and incubated overnight. Next, varying concentrations of RFP, DNA(polyA, polyT)-RFP and CNA(polyA, polyT)-RFP ranging from 0.1 to 100 nM were incubated with the cells for 24 h followed by MTT metabolic assays. As shown in Figure S1, conjugating the protein with either DNA or CNA caused little decrease in cell viability even with protein concentrations as high as 100 nM.

Since neither DNA nor CNA conjugated RFP showed cell toxicity, we next measured protein uptake in MDA-MB-468 cells as a function of incubation time. For this, 1 nM RFP, DNA-RFP and CNA-RFP were added to cells seeded overnight at 37 ºC and incubated for 1-24 h. At specific time points the media was removed and the cells were washed with PBS, trypsinized, and diluted further in PBS for immediate analysis by flow cytometry. As shown in Figure 2a, conjugating CNA to RFP led to an increase in protein uptake as compared to either DNA-RFP or RFP alone. After 24 h the highest amount of protein uptake was seen with polyA-CNA-RFP, which was ~2.5 fold higher than polyA-DNA-RFP. Similarly, polyT-CNA-RFP showed a ~2.3 fold increase over polyT-DNA-RFP. In the case of the DNA conjugated RFP, both polyA and polyT showed similar amounts of protein uptake by the cells, though the yield of DNA-RFP in cells was lower than that of either polyT- or polyA-CNA conjugated RFP. When no oligonucleotides were attached to the proteins, almost no protein uptake was observed. It should be noted however that the act of chemically modifying other proteins with CNA can lead to possible protein denaturation and loss of activity or elicit a immunogenic response during delivery to a targeted site. The flow cytometry studies were also verified qualitatively by confocal imaging after 24h, staining with DAPI and DiO, shown in Figure 2b cells incubated with CNA-RFP showed markedly higher levels of entrapped RFP as compared to either native RFP or DNA-RFP, matching the flow cytometry results. Protein uptake was also tested using CaCo-2 cells, a human epithelial colorectal adenocarcinoma cell line. As with MDA-MB-468 cells, protein uptake of the CNA- and DNA conjugated RFP was enhanced as compared to RFP alone (Figure S2). However, it should be noted that the amount of total protein uptake was less as compared to MDA-MB-468 cells and little difference was seen between CNA-RFP and DNA-RFP. This could be attributed to differences in cell phenotype and cellular uptake processes. Lastly, to compare to either CNA- or DNA-RFP, the cell penetrating TAT peptide was conjugated to RFP via click chemistry (Figure S3). After incubating TAT-RFP with MDA-MB-468 cells for 24 h, flow cytometry showed a 2-fold increase in cell uptake of the TAT-RFP (Figure S4).

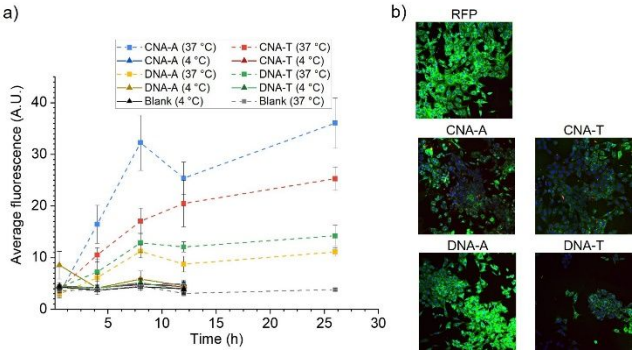

Figure 2. a) Flow cytometry results of MDA-MB-468 cells incubated with 1 nM RFP, DNA-RFP and CNA-RFP at 37 ºC and 4 ºC. The y axis represents the average fluorescence of gated events upon 561nm excitation. b) Confocal images obtained of MDA-MB-468 cells after 24 h incubation with 1 nM RFP, DNA (polyT)-RFP and CNA (polyT)-RFP at 37 ºC, with blue representing DAPI nuclear stain, DiO membrane stain represented in green, and RFP in red. All intensities are treated equally to be comparable.

In order to determine if cell uptake of the CNA-RFP conjugates were occurring by either a passive or active process, the uptake studies were repeated in parallel at 4 ºC, where the low temperature effectively stops all metabolic activity. As shown in Figure 2a, tests with suppressed cell activity show no uptake when compared to the controls, indicating that protein uptake of CNA-RFP is metabolically driven and does not occur by passive diffusion despite the fact that CNA oligonucleotides are neutral in charge and the different solubility profile compared to DNA. Unmodified protein controls show no uptake in the cells, hence it can be deduced the process by which protein uptake occurs can only arise from the oligonucleotide modifications and not by the protein itself (Figure 2a). It must be also noted that at 4 °C the cells start to visibly detach from the wells after ~15 h of incubation.

To identify a possible mechanism by which CNA conjugated proteins were being taken up by the cells, pharmacological inhibitors that either sequestered or bound to specific cell membrane agents were tested. First, inhibitors that bound to cholesterol and scavenger receptors were tested by using methyl-β-cyclodextrin (MBC) and fucoidan, respectively. First, in order to determine inhibitor concentrations to use while avoiding cytotoxicity, MTT assays were run using varying concentrations of fucoidan and MBC (Figures S5 and S6). Next, MDA-MB-468 cells seeded overnight at 50,000 cells/well were incubated with 1 mg/ml of MBC or 10 and 50 µg/ml of fucoidan for 1 h. This was then followed by adding in 1 nM RFP, DNA-RFP or CNA-RFP and incubating further for 24 h before flow cytometry was performed.

As shown in Figure 3A, while the addition of MBC caused little to no decrease in RFP uptake as compared to the control samples (no inhibitor added), the use of fucoidan caused a substantial drop in the detected amounts of both CNA- and DNA-RFP, irrespective of sequence. In addition, using higher concentrations of fucoidan led to a further decrease in uptake of CNA- or DNA-RFP, supporting the hypothesis that scavenger receptors play a strong role in mediating protein uptake. It should be noted that due to the cellular toxicity of MBC, low concentrations of the inhibitor had to be used and this may be in part responsible for the lack of observed changes in protein uptake compared to the control samples.

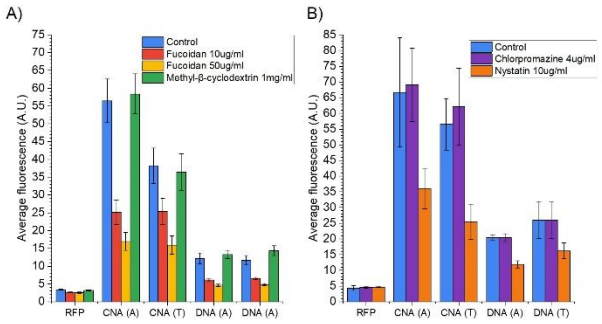

Figure 3. A) Flow cytometry results of the uptake of RFP, DNA-RFP and CNA-RFP to cells treated first with either fucoidan and MBC after 24 h incubation at 37 ºC. Each sample was tested in triplicate. B) Flow cytometry results of RFP, DNA-RFP and CNA-RFP uptake in MDA-MB-468 cells treated with either Chlorpromazine or Nystatin. Each sample was tested in triplicate.

Additionally, chemical inhibitors that disrupt either clathrin or caveolae mediated endocytosis were tested. For this, protein uptake studies with inhibitors were repeated as before by treating cells with either Nystatin or Chlorpromazine, inhibitors of caveolae and clathrin mediated endocytosis respectively.[40–43] MTT assays were also run to determine the appropriate concentrations of inhibitors to use with minimal cell cytotoxicity (Figures S7 and S8). As shown in Figure 3B, while treating the cells with Chlorpromazine led to little to no changes in protein uptake as compared to the control samples, the addition of Nystatin caused a significant decrease in cell uptake of both the CNA- and DNA-RFP. Since scavenger receptors are associated with lipid raft domains and play a dominant role in caveolae-mediated endocytosis, the results obtained with Nystatin support the fucoidan results shown in Figure 3A in that CNA conjugation to proteins most likely occurs via a scavenger receptor and caveolae mediated endocytosis process.

Lastly, co-localization studies were run using the DNA-RFP and CNA-RFP in conjunction with 4 µg/ml FITC-labeled anti-scavenger receptor A antibodies (Thermo, #MA1-81060). For this, MDA-MB-468 cells seeded overnight in imaging plates were incubated with either DNA-RFP or CNA-RFP for 1 h. The cells were washed with PBS and treated with dye-labeled primary anti-SR-A for 15 min. Co-localization analysis was performed on the images from the green and red channels, a heat map of normalized pixel intensities is shown in Figure 4 along with a Pearson Correlation Coefficient (PCC) to provide a measure of the colocalization. It was found that both DNA- and CNA-RFP showed high degrees of colocalization, this greater uptake is consistent with flow cytometry data shown in Figure 2a and Figure 3, and the comparable confocal data in Figure 2b, with the CNA-conjugated proteins showing higher cell uptake than the DNA modified versions because CNA strands have higher binding affinities to scavenger receptor proteins. While scavenger receptors are a diverse group of membrane proteins that recognize a broad spectrum of ligands, from lipoproteins to microbial components,[44] CNA strands may show a preference binding to them due to the interaction between the thiol-rich backbone of the CNA strands and the cysteine rich domains of scavenger receptors.[45,46]

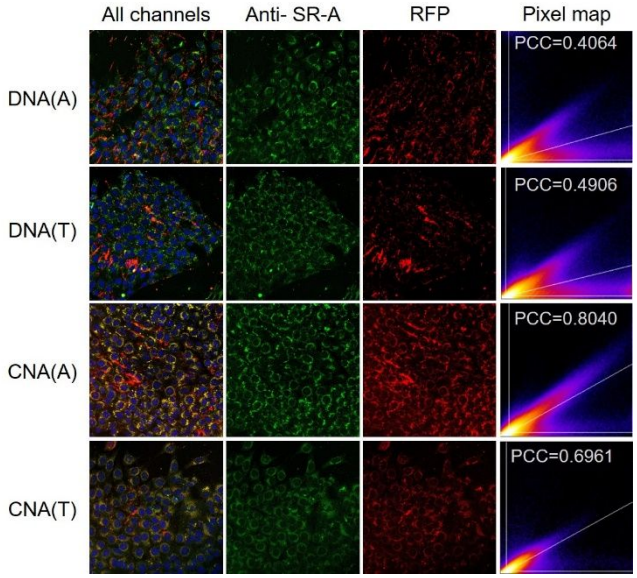

Figure 4. Co-localization confocal images of DNA-RFP and CNA-RFP showing from left to right a merged image of all imaging channels, FITC labelled anti SR-A in the green channel, RFP in the red channel. In the last column, a pixel map of the co-localization images is shown with the corresponding PCC noted on top.

In this work we demonstrated that conjugating proteins with CNAs greatly improves cellular uptake compared to native proteins or proteins modified with analogous amounts and sequences of DNA. In addition, it was demonstrated through comparisons at different temperatures that CNA conjugated proteins followed cell uptake through a metabolically driven process with no measured passive uptake. To further investigate the underlying mechanics, pharmacological inhibitors were tested, suggesting CNA-protein delivery occurred via a pathway dependent on scavenger receptor interactions. Furthermore, when caveolae mediated endocytosis was inhibited in cells, there was a marked decrease in the protein uptake of the MDA-MB-468 cells. Lastly, co-localization studies were performed using a dye-labeled SR-A antibody, showing the highest co-localization levels over a 1 h period occurred with CNA-RFP rather than DNA-RFP.

Conflicts of interest

The authors declare no conflicts of interests.

Notes and references

‡ We gratefully acknowledge financial support from NSF- MRSEC DMR1420736. We are grateful for the technical support provided by Joe Dravagon for confocal microscopy, Theresa Stines and S10OD021601 for FACS, Srijit Mukherjee for providing the mScarlet strains and Shambojit Roy and Saheli Ganguly for support in cell culturing.

1 C. O. Weill, S. Biri, A. Adib and P. Erbacher, *Cytotechnology*, 2008, **56**, 41–48.
2 K. A. Andersen, T. P. Smith, J. E. Lomax and R. T. Raines, *ACS Chem. Biol.*, 2016, **11**, 319–323.
3 D. S. D'Astolfo, R. J. Pagliero, A. Pras, W. R. Karthaus, H. Clevers, V. Prasad, R. J. Lebbink, H. Rehmann and N. Geijsen, *Cell*, 2015, **161**, 674–690.
4 V. J. Bruce and B. R. McNaughton, *Cell Chem. Biol.*, 2017, **24**, 924–934.
5 A. Fu, R. Tang, J. Hardie, M. E. Farkas and V. M. Rotello, *Bioconjug. Chem.*, 2014, **25**, 1602–1608.
6 Y. Lee, D. C. Luther, J. A. Kretzmann, A. Burden, T. Jeon, S. Zhai and V. M. Rotello, *Theranostics*, 2019, **9**, 3280–3292.
7 B. Leader, Q. J. Baca and D. E. Golan, *Nat. Rev. Drug Discov.*, 2008, **7**, 21–39.
8 Z. Gu, A. Biswas, M. Zhao and Y. Tang, *Chem. Soc. Rev.*, 2011, **40**, 3638.
9 A. Harguindey, S. Roy, A. W. Harris, B. D. Fairbanks, A. P. Goodwin, C. N. Bowman and J. N. Cha, *Biomacromolecules*, 2019, **20**, 1683–1690.
10 A. L. Z. Lee, Y. Wang, W. Ye, H. S. Yoon, S. Y. Chan and Y. Yang, *Biomaterials*, 2008, **29**, 1224–1232.
11 H. Zhao, Z. Y. Lin, L. Yildirimer, A. Dhinakar, X. Zhao and J. Wu, *J. Mater. Chem. B*, 2016, **4**, 4060–4071.
12 M. Chou, H. Yu, J. Hsia, Y. Chen, T. Hung, H.-M. Chao, E. Chern and Y.-Y. Huang, *Materials (Basel).*, 2018, **11**, 301.
13 M. Furuhata, H. Kawakami, K. Toma, Y. Hattori and Y. Maitani, *Bioconjug. Chem.*, 2006, **17**, 935–942.
14 B. Chatin, M. Mével, J. Devallière, L. Dallet, T. Haudebourg, P. Peuziat, T. Colombani, M. Berchel, O. Lambert, A. Edelman and B. Pitard, *Mol. Ther. - Nucleic Acids*, 2015, **4**, e244.
15 C. Liu, T. Wan, H. Wang, S. Zhang, Y. Ping and Y. Cheng, *Sci. Adv.*, 2019, **5**, eaaw8922.
16 C. Bechara and S. Sagan, *FEBS Lett.*, 2013, **587**, 1693–1702.
17 A. El-Sayed, S. Futaki and H. Harashima, *AAPS J.*, 2009, **11**, 13–22.
18 V. J. Bruce, M. Lopez-Islas and B. R. McNaughton, *Protein Sci.*, 2016, **25**, 1129–1137.
19 R. Brock, *Bioconjug. Chem.*, 2014, **25**, 863–868.
20 S. J. Kaczmarczyk, K. Sitaraman, H. A. Young, S. H. Hughes and D. K. Chatterjee, *Proc. Natl. Acad. Sci.*, 2011, **108**, 16998–17003.
21 E. Mahon, A. Salvati, F. Baldelli Bombelli, I. Lynch and K. A. Dawson, *J. Control. Release*, 2012, **161**, 164–174.
22 F. Danhier, E. Ansorena, J. M. Silva, R. Coco, A. Le Breton and V. Préat, *J. Control. Release*, 2012, **161**, 505–522.
23 G. Crotts and T. G. Park, *J. Microencapsul.*, 1998, **15**, 699–713.
24 V. J. Bruce and B. R. McNaughton, *Cell Chem. Biol.*, 2017, **24**, 924–934.
25 B. R. McNaughton, J. J. Cronican, D. B. Thompson and D. R. Liu, *Proc. Natl. Acad. Sci.*, 2009, **106**, 6111–6116.
26 S. M. Fuchs and R. T. Raines, *ACS Chem. Biol.*, 2007, **2**, 167–170.
27 D. Bar-Sagi and J. R. Feramisco, *Cell*, 1985, **42**, 841–848.
28 W. Chen, H. Li, D. Shi, Z. Liu and W. Yuan, *Front. Pharmacol.*, , DOI:10.3389/fphar.2016.00137.
29 K. Krishnamoorthy, K. Hoffmann, S. Kewalramani, J. D. Brodin, L. M. Moreau, C. A. Mirkin, M. Olvera de la Cruz and M. J. Bedzyk, *ACS Cent. Sci.*, 2018, **4**, 378–386.
30 J. D. Brodin, A. J. Sprangers, J. R. McMillan and C. A. Mirkin, *J. Am. Chem. Soc.*, 2015, **137**, 14838–14841.
31 C. H. J. Choi, L. Hao, S. P. Narayan, E. Auyeung and C. A. Mirkin, *Proc. Natl. Acad. Sci.*, 2013, **110**, 7625–7630.
32 J. I. Cutler, E. Auyeung and C. A. Mirkin, *J. Am. Chem. Soc.*, 2012, **134**, 1376–1391.
33 S. N. Barnaby, T. L. Sita, S. H. Petrosko, A. H. Stegh and C. A. Mirkin, in *Nanotechnology-Based Precision Tools for the Detection and Treatment of Cancer*, 2015, pp. 23–50.
34 W. Xi, S. Pattanayak, C. Wang, B. Fairbanks, T. Gong, J. Wagner, C. J. Kloxin and C. N. Bowman, *Angew. Chemie Int. Ed.*, 2015, **54**, 14462–14467.
35 A. Harguindey, D. W. Domaille, B. D. Fairbanks, J. Wagner, C. N. Bowman and J. N. Cha, *Adv. Mater.*, 2017, **29**, 1700743.
36 Z. Liu, B. Fairbanks, L. He, T. Liu, P. Shah, J. N. Cha, J. W. Stansbury and C. N. Bowman, *Chem. Commun.*, 2017, **53**, 10156–10159.
37 X. Han, D. W. Domaille, B. D. Fairbanks, L. He, H. R. Culver, X. Zhang, J. N. Cha and C. N. Bowman, *Biomacromolecules*, 2018, **19**, 4139–4146.
38 A. J. Anderson, E. B. Peters, A. Neumann, J. Wagner, B. Fairbanks, S. J. Bryant and C. N. Bowman, *Biomacromolecules*, 2018, acs.biomac.8b00162.
39 D. S. Bindels, L. Haarbosch, L. van Weeren, M. Postma, K. E. Wiese, M. Mastop, S. Aumonier, G. Gotthard, A. Royant, M. A. Hink and T. W. J. Gadella, *Nat. Methods*, 2017, **14**, 53–56.
40 K. M. Hussain, K. L. J. Leong, M. M. Ng and J. J. H. Chu, *J. Biol. Chem.*, 2011, **286**, 309–321.
41 X. Zhu, Y. Zhuang, J. Ben, L. Qian, H. Huang, H. Bai, J. Sha, Z.-G. He and Q. Chen, *J. Biol. Chem.*, 2011, **286**, 8231–8239.
42 F. Chen, L. Zhu, Y. Zhang, D. Kumar, G. Cao, X. Hu, Z. Liang, S. Kuang, R. Xue and C. Gong, *Sci. Rep.*, 2018, **8**, 7268.
43 F. Zhang, H. Guo, J. Zhang, Q. Chen and Q. Fang, *Virology*, 2018, **513**, 195–207.
44 X. Yu, C. Guo, P. B. Fisher, J. R. Subjeck and X.-Y. Wang, in *Advances in Cancer Research*, Elsevier Inc., 1st edn., 2015, vol. 128, pp. 309–364.
45 E. Hohenester, T. Sasaki and R. Timpl, *Nat. Struct. Biol.*, 1999, **6**, 228–232.
46 N. V. L. Yap, F. J. Whelan, D. M. E. Bowdish and G. B. Golding, *Front. Immunol.*, 2015, **6**, 1–9.

